Multi-scale modelling of elastic waves. Theoretical justification and numerical simulation of band gaps

A. Avila, Georges Griso, Bernadette Miara, E. Rohan

Multi-scale modelling of elastic waves
Theoretical justification and numerical simulation of band gaps

A. Ávila, G. Griso, B. Miara, E. Rohan

Universidad de La Frontera, Avenida Francisco Salazar, 01145 Temuco, Chile
Université Pierre et Marie Curie, Laboratoire Jacques-Louis Lions, 4, Place Jussieu, 75252 Paris, France
Laboratoire de Modélisation et Simulation Numérique, ESIEE, 2, boulevard Blaise Pascal, 93160 Noisy-le-Grand, France
Department of Mechanics, Faculty of Applied Sciences, University of West Bohemia, Plzeň, Czech Republic

E-mail: aavila@ufro.cl, georges.griso@wanadoo.fr, miarab@esiee.fr, rohan@kme.zcu.cz

Keywords: elastic waves; composite materials; strong heterogeneities; homogenization; negative mass density; band gaps.

Abstract

We consider a three-dimensional composite material made of small inclusions periodically embedded in an elastic matrix, the whole structure presents strong heterogeneities between its different components. In the general framework of linearized elasticity we show that, when the size of the microstructures tends to zero, the limit homogeneous structure presents, for some wavelengths, a negative mass density tensor. Hence we are able to rigorously justify the existence of forbidden bands, i.e., intervals of frequencies in which there is no propagation of elastic waves. In particular, we show how to compute these band gaps and we illustrate the theoretical results with some numerical simulations.

1 Introduction

After the huge impact due to the development of photonic crystals [10, 14], the development of phononic crystals has received growing interest in recent years. These artificial crystals, which mimic a crystalline atomic lattice, are structured materials formed of *periodic microstructures*. In the case of phononic crystals considered by Vasseur and al. [13], the media is a two-dimensional binary solid-solid composite made of elastic arrays of Duralumin cylindrical inclusions embedded in a resin epoxy matrix. For this structure, measured transmission exhibit absolute acoustic band gaps. A band gap is a range of frequency in which elastic or acoustic waves cannot propagate; it is surrounded, above and below, by propagating states.

From a *technological point of view* the main interest of these composites is to help reduce the noise level, they are also good candidates for the design of elastic or acoustic waveguides or filters.

From a *mathematical point of view*, the homogenization approach (which consists in replacing a composite by a limit homogeneous material) is relevant for the modelling of such periodic structures. Let us note that the property for a periodic structure to always present band gaps (Floquet-Bloch's theory), disappears in the case of an homogeneous material. However, the asymptotic analysis shows that in the case of photonic crystals the limit "homogeneous permeability" is *negative* for certain wavelengths and hence band gaps appear [4]. In the case of phononic crystals our study aims at justifying the existence of band gaps for certain wavelengths; this result is a consequence of the non positivity of the limit "homogeneous mass density". The homogenization method we use to obtain this result relies on the unfolding method [5] that combines the dilatation technique with ideas from finite element approximations.

From a *numerical point of view* some computational works have been developed to optimize the shape of the inclusions [7, 12] with a classical approach (different from ours which is based on the micro-macro study). For the time being, we present in this paper the numerical simulation of the band gaps, with an emphasis on *weak band gaps* (propagation in certain directions only) and *strong band gaps* (no propagation in any directions). Further studies on the sensitivity analysis of these forbidden bands are under preparation [11, 9].

To present the problem under study let us start with the description of the geometry of the composite whose reference configuration $\overline{\Omega}$ of the elastic body is supposed to be stress-free. The bounded domain $\Omega \subset \mathbb{R}^3$ with micro structures of size $\varepsilon > 0$, is split into a domain Ω_1^ε occupied by the matrix made of material 1, and a domain Ω_2^ε (with Lipschitz-continuous boundary denoted by $\partial\Omega$) which contains periodically distributed inclusions made of material 2, hence $\Omega = \Omega_1^\varepsilon \cup \Omega_2^\varepsilon$ with $\Omega_1^\varepsilon \cap \Omega_2^\varepsilon = \emptyset$. We note that the whole domain Ω is independent of ε, whereas the domains occupied by the matrix and the inclusions are both ε-dependent. As for the study of three-dimensional periodic structure, let us introduce the reference cell $Y = [0,1[^3$ with its elementary inclusion Y_2 , $\overline{Y_2} \subset Y, \quad Y_1 = Y \backslash \overline{Y_2}$. Therefore, material 2 occupies the domain Ω_2^ε obtained by ε-periodicity and material 1 occupies the remaining domain, $\Omega_1^\varepsilon = \Omega \backslash \overline{\Omega_2^\varepsilon}$:

$$\Omega_2^\varepsilon = \bigcup_{k \in \mathbb{K}^\varepsilon} \varepsilon(\overline{Y_2} + k), \quad \mathbb{K}^\varepsilon = \{k \in \mathbb{Z}^3, \varepsilon(\overline{Y_2} + k) \subset \Omega\}.$$

Let us denote by $\boldsymbol{u}^\varepsilon(\omega)$ the static elastic displacement field that the body undergoes at a *fixed wavelength* ω (the displacement is indexed by ε since, obviously, it depends on the microstructure size ε). Our paper deals with the convergence of the sequence $\{\boldsymbol{u}^\varepsilon(\omega)\}_\varepsilon$ when ε goes to zero. In section 2 we recall the propagation equations for elastic waves solved by $\boldsymbol{u}^\varepsilon(\omega)$ for positive values of ε. In section 3 we introduce the unfolding operator and give its essential properties so that we are in a position, in section 4, to establish the main convergence theorem which gives the propagation equations solved by the limit displacement field $\boldsymbol{u}(\omega)$. In section 5 we discuss the possibility of a "negative" mass density and its consequence for the existence of forbidden propagation bands. All the proofs of the existence and convergence theorems are given in section 6. Finally, in section 7, numerical simulations illustrate the influence of the change of some parameters of the micro structures (such as shape of the inclusions, average mass density of the composite, fill-in coefficient).

2 Propagation of elastic waves

In this section we recall the equations of the elastic waves propagation in the composite material described previously and next we give the equilibrium equations in the static case with fixed wavelength.
Let $T > 0$; under the action of applied forces[1] $\boldsymbol{F} = (F_m) : \Omega \times (0,T) \to \mathbb{R}^3$ the body undergoes an elastic displacement field $\boldsymbol{U}^\varepsilon = (U_m^\varepsilon) : \overline{\Omega} \times (0,T) \to \mathbb{R}^3$ which is solution to the evolution problem:

$$\left\{ \begin{array}{ll} r^\varepsilon(x)\dfrac{\partial^2}{\partial t^2}U_m^\varepsilon(x,t) - \dfrac{\partial}{\partial x_n}(c^\varepsilon_{mnkl}(x)e_{kl}(\boldsymbol{U}^\varepsilon(x,t))) = F_m & \text{in} \quad \Omega \times (0,\mathrm{T}), \\ \boldsymbol{U}^\varepsilon(x,t) = \boldsymbol{0} & \text{on} \quad \partial\Omega \times (0,\mathrm{T}), \\ \boldsymbol{U}^\varepsilon(x,0) = \boldsymbol{U}^0(x), \quad \dfrac{\partial}{\partial t}\boldsymbol{U}^\varepsilon(x,0) = \boldsymbol{U}^1(x) & \text{in} \quad \Omega, \end{array} \right.$$

with initial conditions $\boldsymbol{U}^0 : \overline{\Omega} \to \mathbb{R}^3, \boldsymbol{U}^1 : \overline{\Omega} \to \mathbb{R}^3$ and where

$$e_{kl}(\boldsymbol{V}(x,t)) = \frac{1}{2}(\partial_k V_l(x,t) + \partial_l V_k(x,t)),$$

is the linearized deformation tensor.
The mass density $r^\varepsilon : \overline{\Omega} \longrightarrow \mathbb{R}$ and the elasticity tensor of the structure $c^\varepsilon = (c^\varepsilon_{mnkl})$, with $c^\varepsilon_{mnkl} : \overline{\Omega} \longrightarrow \mathbb{R}$ possess the classical properties of any elastic body:
-There exists two positive constants $\rho^\varepsilon_-, \rho^\varepsilon_+$ such that:

$$\rho^\varepsilon_- \leq r^\varepsilon(x) \leq \rho^\varepsilon_+ \text{ for all } x \in \Omega.$$

-The elasticity tensor is symmetric and coercive, i.e., :

$$c^\varepsilon_{klmn} = c^\varepsilon_{mnkl} = c^\varepsilon_{nmlk},$$

and there exists $\alpha^\varepsilon > 0, \beta^\varepsilon > 0$ such that, for any symmetric matrix (X_{mn}), we have

$$\alpha^\varepsilon X_{mn}X_{mn} \leq c^\varepsilon_{mnkl}(x)X_{mn}X_{kl} \leq \beta^\varepsilon X_{mn}X_{mn} \text{ for all } x \in \Omega.$$

For any fixed $\varepsilon > 0$, and standard assumptions on the regularity of the data

$$r^\varepsilon \in L^2(\Omega), c^\varepsilon_{mnkl} \in L^2(\Omega), \boldsymbol{F} \in \boldsymbol{L}^2(\Omega \times (0,T)), \boldsymbol{U}^0 \in \boldsymbol{H}^1_0(\Omega), \boldsymbol{U}^1 \in \boldsymbol{L}^2(\Omega),$$

the associated variational problem has a unique weak solution

$$\boldsymbol{U}^\varepsilon \in \boldsymbol{C}(0,T;\boldsymbol{H}^1_0(\Omega)), \frac{\partial}{\partial t}\boldsymbol{U}^\varepsilon \in \boldsymbol{C}(0,T;\boldsymbol{L}^2(\Omega)).$$

Let us now consider an incident wave period ω *fixed and independent of* ε, and the periodic solution $\boldsymbol{U}^\varepsilon(x,t) = \boldsymbol{u}^\varepsilon(x,\omega)e^{i\omega t}$ associated to periodic applied forces $\boldsymbol{F}(x,t) = \boldsymbol{f}(x)e^{i\omega t}$ and compatible initial conditions; in the sequel we denote by $\boldsymbol{u}^\varepsilon(x)$, instead of

[1] Latin exponents and indices take their values in the set $\{1,2,3\}$. Einstein convention for repeated exponents and indices is used. Bold face letters represent vectors or vector spaces.

$\boldsymbol{u}^\varepsilon(x,\omega)$, *the amplitude of the elastic wave*.
Hence, for any fixed $\varepsilon > 0$, the elastic field $\boldsymbol{u}^\varepsilon : \overline{\Omega} \to \mathbb{C}^3$ is given by the stationary problem,

$$\left\{ \begin{array}{ll} \omega^2 r^\varepsilon(x) u_m^\varepsilon(x) + \partial_n(c_{mnkl}^\varepsilon(x) e_{kl}(\boldsymbol{u}^\varepsilon(x))) = -f_m & \text{in} \quad \Omega, \\ \boldsymbol{u}^\varepsilon(x) = \mathbf{0} & \text{on} \quad \partial\Omega. \end{array} \right.$$

Because of the linearity of the problem, we consider in the sequel only real-valued displacement field $\boldsymbol{u}^\varepsilon : \overline{\Omega} \to \mathbb{R}^3$. According to Fredholm alternative, for each fixed value of ω different from the resonance values (square root of the eigenvalues of the elasticity problem) which *depend upon* ε, the variational problem:

$$\omega^2 \int_\Omega r^\varepsilon \boldsymbol{u}^\varepsilon \cdot \Phi - \int_\Omega c_{mnkl}^\varepsilon e_{kl}(\boldsymbol{u}^\varepsilon) e_{mn}(\Phi) = -\int_\Omega \boldsymbol{f} \cdot \Phi \quad \forall \Phi \in \boldsymbol{H}_0^1(\Omega). \qquad (1)$$

(where $\boldsymbol{u} \cdot \boldsymbol{v} = u_k v_k$) has a unique solution $\boldsymbol{u}^\varepsilon \in \boldsymbol{H}_0^1(\Omega)$.

The rest of the paper aims, first of all, at showing that the sequence $\{\boldsymbol{u}^\varepsilon\}_\varepsilon$ of solutions to (1) converges (in a certain sense that will be made more precise later) to the solution of an homogeneous problem, and next at interpreting the theoretical and numerical properties of this limit solution.

3 Unfolding operator and heterogeneities

3.1 Definitions and basic properties of the unfolding operator

In conjunction with the elementary cell Y, there exists, for all $z \in \mathbb{R}^3$, a unique decomposition $z = [z] + \{z\}$ with an integer part $[z]$ and a remaining part $\{z\}$ such that $\{z\} = z - [z] \in Y$ and equivalently, we have the unique decomposition $z = \varepsilon[\frac{z}{\varepsilon}] + \varepsilon\{\frac{z}{\varepsilon}\}$.

We introduce the unfolding operator $\mathcal{T}^\varepsilon$ related to the study of periodic structures [5, 6]. For all $v \in L^2(\Omega)$ extended by 0 outside Ω :

$$\mathcal{T}^\varepsilon : v \in L^2(\Omega) \longrightarrow \mathcal{T}^\varepsilon(v)(x,y) = v(\varepsilon[\frac{x}{\varepsilon}] + \varepsilon y), \quad x \in \Omega, y \in Y.$$

The main properties of this operator are given below (complete proofs can be found in [5]).
• If $\{v^\varepsilon\}_\varepsilon$ is uniformly bounded in $L^2(\Omega)$ then, there exists $v \in L^2(\Omega \times Y)$ such that, up to subsequence still denoted with the same indices, we have the convergence: $\mathcal{T}^\varepsilon(v^\varepsilon) \rightharpoonup v$ weakly in $L^2(\Omega \times Y)$.
• If the sequence $\{v^\varepsilon\}_\varepsilon$ is uniformly bounded in $L^2(\Omega)$ and the sequence $\{\varepsilon \nabla v^\varepsilon\}_\varepsilon$ is uniformly bounded in $L^2(\Omega; \mathbb{R}^3)$ then, there exists a limit field $v \in L^2(\Omega; H^1_{\text{per}}(Y))$ such that, up to subsequences still denoted with the same indices, we have the convergence:

$$\left\{ \begin{array}{lll} \mathcal{T}^\varepsilon(v^\varepsilon) & \rightharpoonup v & \text{weakly in } L^2(\Omega \times Y), \\ \mathcal{T}^\varepsilon(\varepsilon \nabla_x v^\varepsilon) & \rightharpoonup \nabla_y v & \text{weakly in } L^2(\Omega \times Y; \mathbb{R}^3), \end{array} \right.$$

where $\nabla_x v = \Big(\dfrac{\partial v(x,y)}{\partial x_i}\Big)_{1 \le i \le 3}$ and $\nabla_y v = \Big(\dfrac{\partial v(x,y)}{\partial y_i}\Big)_{1 \le i \le 3}$.
• If $\{v^\varepsilon\}_\varepsilon$ is uniformly bounded in $H^1(\Omega)$ then, there exists a limit field $v \in H^1(\Omega)$ and

a corrector $\overline{v} \in L^2(\Omega, H^1_{\rm per}(Y))$ such that, up to subsequences still denoted with the same indices, we have the convergence:

$$\left\{\begin{array}{lll} v^\varepsilon & \rightharpoonup v & \text{weakly in } H^1(\Omega), \\ \mathcal{T}^\varepsilon(v^\varepsilon) & \rightharpoonup v & \text{weakly in } L^2(\Omega \times Y), \\ \mathcal{T}^\varepsilon(\nabla_x v^\varepsilon) & \rightharpoonup \nabla_x v + \nabla_y \overline{v} & \text{weakly in } L^2(\Omega \times Y; \mathbb{R}^3). \end{array}\right.$$

Periodic problems have also been studied by the two-scale method [1, 8]

3.2 Heterogeneities

We are now in a position to state the dependence of the materials characteristics in terms of ε. When these characteristics are not scaled by ε the limit homogeneous model does not exhibit band gaps. Since we are interested by the modelling of the bad gap structure we assume in the sequel that there exists new functions r_1, r_2, c_1, c_2 independent of the size ε of the micro structures such that:

$$\left\{\begin{array}{lll} \text{(In the matrix)} & r^\varepsilon(x) = r_1(\{\frac{x}{\varepsilon}\}), \quad c^\varepsilon_{mnkl}(x) = c_{1,mnkl}(\{\frac{x}{\varepsilon}\}) & x \in \Omega_1^\varepsilon, \\ \text{(In the inclusions)} & r^\varepsilon(x) = r_2(\{\frac{x}{\varepsilon}\}), \quad c^\varepsilon_{mnkl}(x) = \varepsilon^2 c_{2,mnkl}(\{\frac{x}{\varepsilon}\}) & x \in \Omega_2^\varepsilon. \end{array}\right.$$

in other words, functions r_1, r_2, c_1, c_2 are defined in the elementary cell Y by the relations,

$$\left\{\begin{array}{ll} \mathcal{T}^\varepsilon(r^\varepsilon)(x,y) = r_1(y), \quad \mathcal{T}^\varepsilon(c^\varepsilon_{mnkl})(x,y) = c_{1,mnkl}(y), & x \in \Omega_1^\varepsilon, y \in Y_1, \\ \mathcal{T}^\varepsilon(r^\varepsilon)(x,y) = r_2(y), \quad \mathcal{T}^\varepsilon(c^\varepsilon_{mnkl})(x,y) = \varepsilon^2 c_{2,mnkl}(y), & x \in \Omega_2^\varepsilon, y \in Y_2. \end{array}\right.$$

The scaling ε^2, which appears in front of the elasticity tensor, is the expression of the *strong heterogeneity* that exists between the elastic properties of the matrix and that of the inclusions ones. Different kinds of scalings are possible, however this scaling is the only one that gives rise to a limit model with significant physical meanings (in this direction, see [1] and [2] where an example for which this type of assumption is used to solve a double porosity problem). This scaling and the continuity and coercivity constants introduced in Section 3.1 now read: There exists positive constants $\rho_-, \rho_+, \alpha, \beta$ independent of ε such that:

$$\rho_- \leq r_1(y) \leq \rho_+ \text{ for all } y \in Y_1, \quad \rho_- \leq r_2(y) \leq \rho_+ \text{ for all } y \in Y_2,$$

and such that, for all symmetric matrix (X_{mn}), we have:

$$\alpha X_{mn} X_{mn} \leq c_{1,mnkl}(y) X_{mn} X_{kl} \leq \beta X_{mn} X_{mn} \text{ for all } y \in Y_1,$$

and the same property holds for the elasticity tensor c_2,

$$\alpha X_{mn} X_{mn} \leq c_{2,mnkl}(y) X_{mn} X_{kl} \leq \beta X_{mn} X_{mn} \text{ for all } y \in Y_2.$$

4 The limit problem

We recall that the solution $\boldsymbol{u}^\varepsilon$ to (1) exists for all frequencies ω different from resonance values (which depend upon ε). Therefore, before showing that when the size ε of the micro structures in the composite goes to zero the sequence $\{\boldsymbol{u}^\varepsilon\}_\varepsilon$ converges to the solution of limit problem, we show that there exist an admissible set of frequencies W (independent of ε) such that $\{\boldsymbol{u}^\varepsilon\}_\varepsilon$ exists for all frequencies in W for ε small enough. However this is not possible for all structures, hence we have to restrict our study to a class of structures *which allow limit wave propagation*.

Assumption on the data. We assume that the density r_2, the elastic characteristics c_2 and the geometry of the elementary inclusion Y_2 and the density r_1 assure the *existence of a non empty open set of frequencies* $W \subset \mathbb{R}^+$ (this will be made more precise in Step 7 of Section 6), that allows us to prove the existence of a solution to (1) for all frequency $\omega \in W$ and next its convergence to the solution of a limit problem.

Existence Theorem 1. For all $\omega \in W$, there exists a positive value $\varepsilon_0(\omega)$ such that, for all $\varepsilon \in]0, \varepsilon_0(\omega)]$ problem (1) has a unique solution bounded in $\boldsymbol{L}^2(\Omega)$.
The proof, for the sake of clarity, is postponed to Step 7 of Section 6.

Convergence Theorem 2. *For all values of the incident wave $\omega \in W$ there exists two limit vector fields $\boldsymbol{u}^1 \in \boldsymbol{H}_0^1(\Omega), \boldsymbol{u}^2 \in \boldsymbol{L}^2(\Omega; \boldsymbol{H}_0^1(Y_2))$ such that:*
(i) The sequence $\mathcal{T}^\varepsilon(\boldsymbol{u}^\varepsilon)$ strongly converges to $\boldsymbol{u} = \boldsymbol{u}^1 + \boldsymbol{u}^2$ in $\boldsymbol{L}^2(\Omega \times Y)$.
(ii) The limit $\boldsymbol{u}^1 \in \boldsymbol{H}_0^1(\Omega)$ is the unique solution to the variational problem:

$$\begin{aligned} \omega^2 \int_\Omega A^*(\omega)\boldsymbol{u}^1(x) \cdot \Phi(x)dx - \int_\Omega c^*_{mnkl} e_{kl}(\boldsymbol{u}^1(x)) e_{mn}(\Phi(x))dx \\ = -\int_\Omega B^*(\omega)\boldsymbol{f}(x) \cdot \Phi(x)dx \qquad \forall \Phi \in \boldsymbol{H}_0^1(\Omega), \end{aligned} \tag{2}$$

where the homogenized elasticity tensor c^*, the homogenized generalized mass density matrix $A^*(\omega)$ *and* the homogenized matrix $B^*(\omega)$ *are given in* (6) *and* (9) *below in section* 6.
(iii) The limit displacement field $\boldsymbol{u}^2 \in \boldsymbol{L}^2(\Omega; \boldsymbol{H}_0^1(Y_2))$ is the unique solution to the variational problem:

$$\begin{aligned} \omega^2 \int_{Y_2} r_2(y)\boldsymbol{u}^2(x,y) \cdot \overline{\Psi}(y)dy - \int_{Y_2} c_{2,mnkl}(y) e_{kl,y}(\boldsymbol{u}^2(x,y)) e_{mn,y}(\overline{\Psi}(y))dy \\ = -\omega^2 \boldsymbol{u}^1(x) \cdot \int_{Y_2} r_2(y)\overline{\Psi}(y)dy - \boldsymbol{f}(x) \cdot \int_{Y_2} \overline{\Psi}(y)dy \qquad \forall \overline{\Psi} \in \boldsymbol{H}_0^1(Y_2). \end{aligned} \tag{3}$$

The existence of a unique solution $\boldsymbol{u}^1$ to problem (2) is proved in Step 4, Lemma 3 of Section 6, the existence of a unique solution $\boldsymbol{u}^2$ to problem (3) is proved in Step 3 of Section 6.

Problem (2) has the same form as problem (1). However it is important to notice that the mass density scalar r^ε has been replaced by the homogenized tensor $A^*(\omega)$ which depends upon the wavelength considered ω, and that the elasticity tensor $c^* = (c^*_{mnkl})$ is now homogeneous and independent of ω.

5 Negative mass density and band-gaps

In view of the limit model given by the solution of problem (2), the propagation of waves in the homogenized structure that occupies the domain Ω depends on the structure of the "mass density matrix" $A^*(\omega)$. Therefore we begin by the examination of its properties in order to prove the existence of the elastic band-gaps, and next we introduce the notion of the so-called *weak* or *strong* band-gaps specially suitable for applications.

5.1 Properties of the homogenized "mass density matrix" $A^*(\omega)$

Let us first give the expression of A^* (that will be justified in Step 3 of section 6),

$$A^*(\omega) = \sum_{j\in J} A^{*,j}(\omega) + r^* I, \quad r^* = \int_{Y_1} r_1(y)dy + \int_{Y_2} r_2(y)dy.$$

The elements of each matrix $A^{*,j} = (A^{*,j}_{pq})$ are given by:

$$A^{*,j}_{pq}(\omega) = \frac{-\omega^2}{\omega^2 - \lambda^j} \int_{Y_2} r_2(y)\varphi^j_p(y) \int_{Y_2} r_2(y)\varphi^j_q(y),$$

where $\{\varphi^j, \lambda^j\}_{j\geq 1}$ are the eigenelements associated to the elasticity operator (r_2, c_2) posed in the domain Y_2, see equation (7) below, and $J = \{j \geq 1, \int_{Y_2} r_2(y)\varphi^j(y)dy \neq 0\}$.

Hence, matrix $A^*(\omega)$ is symmetric, its eigenvalues are real; however when this matrix is not positive definite (i.e., when it has at least one negative eigenvalue), the limit problem may have *evanescent solutions* which means that there is *no wave propagation* in certain directions corresponding to any linear combination of eigenvectors associated to the negative eigenvalues.

The *sign of eigenvalues* of matrix $A^*(\omega)$ will now be investigated in each elementary interval $]\sqrt{\lambda^j}, \sqrt{\lambda^{j+1}}[$. The smallest eigenvalue $\mu_\nabla(\omega)$ is given by the

infimum of the function $\boldsymbol{z} \rightarrow A^*(\omega)\boldsymbol{z}\cdot\boldsymbol{z}$ with $\boldsymbol{z} = (z_p) \in \mathbb{R}^3$ and $||\boldsymbol{z}|| = 1$,

$$\mu_\nabla(\omega) = \inf_{||\boldsymbol{z}||=1} \Big(\sum_{j\in J} \frac{-\omega^2}{\omega^2 - \lambda^j} \sum_{p=1}^{3} \Big(z_p \int_{Y_2} r_2(y)\varphi_p^j(y) \Big)^2 \Big) + r^*.$$

For any $j \in J$, the function $\omega \rightarrow \mu_\nabla(\omega)$ is strictly increasing in the interval $]\sqrt{\lambda^j}, \sqrt{\lambda^{j+1}}[$. We can distinguish the following two cases: either λ^j is of order of multiplicity equal to one, or it is of order of multiplicity greater than one (this situation happens, for example, when the inclusions present geometrical symmetries).

• In the first case, matrix $A^{*,j}(\omega)$ is of rank one, hence the infimum of $A^{*,j}(\omega)\boldsymbol{z}\cdot\boldsymbol{z}$ vanishes. Since in each interval $]\sqrt{\lambda^j}, \sqrt{\lambda^{j+1}}[$ all quantities $A^{*,k}(\omega)\boldsymbol{z}\cdot\boldsymbol{z}$ are bounded for all $k \neq j$, we infer that the smallest eigenvalue increases from $-\infty$ to a finite value $\mu_\nabla^j = \mu_\nabla(\sqrt{\lambda^{j+1}})$. If this value μ_∇^j is non negative, there exists a value $\omega_\nabla^j \in]\sqrt{\lambda^j}, \sqrt{\lambda^{j+1}}[$ such that $\mu_\nabla(\omega_\nabla^j) = 0$, hence $]\sqrt{\lambda^j}, \omega_\nabla^j[$ is a band gap in the sense that it may happen that some waves are not *progressive*. By contrast, in the interval $]\omega_\nabla^j, \sqrt{\lambda^{j+1}}[$ all waves propagate. If μ_∇^j is strictly negative then the whole interval $]\sqrt{\lambda^j}, \sqrt{\lambda^{j+1}}[$ is a forbidden band.

• In the second case, λ^j is of order of multiplicity $M > 1$ and $(\varphi^{j,m})_{m=1,M}$ are the associated eigenvectors. Matrix $A^{*,j}(\omega) = (A_{pq}^{*,j}(\omega))$ is given by:

$$A_{pq}^{*,j}(\omega) = \frac{-\omega^2}{\omega^2 - \lambda^j} \sum_{m=1}^{M} \int_{Y_2} r_2(y)\varphi_p^{j,m}(y) \int_{Y_2} r_2(y)\varphi_q^{j,m}(y).$$

If matrix $A^{*,j}(\omega)$ is of full rank, (contrary to the previous case), $\mu_\nabla(\omega)$ increases from $-\infty$ to $+\infty$, and there always exists a value $\omega_\nabla^j \in]\sqrt{\lambda^j}, \sqrt{\lambda^{j+1}}[$ such that $\mu_\nabla(\omega_\nabla^j) = 0$. In other words there always exists a band gap $]\sqrt{\lambda^j}, \omega_\nabla^j[$. In the case where matrix $A^{*,j}(\omega)$ is not of full rank the behavior of its eigenvalue is the same as in the previous case, i.e., bounded at $\omega = \sqrt{\lambda^{j+1}}$.

To sum up, in each interval $]\sqrt{\lambda^j}, \sqrt{\lambda^{j+1}}[$, the smallest eigenvalue of $A^*(\omega)$ takes negative values in each intervals $]\sqrt{\lambda^j}, \omega_\nabla^j[$, with possibly $\omega_\nabla^j = \sqrt{\lambda^{j+1}}$; in this last case, the band gap extends to the whole interval $]\sqrt{\lambda^j}, \sqrt{\lambda^{j+1}}[$.

By the same way, we establish that the largest eigenvalue $\mu_\Delta(\omega)$ given by the supremum of the same function $\boldsymbol{z} \rightarrow A^*(\omega)\boldsymbol{z}\cdot\boldsymbol{z}, \boldsymbol{z} \in \mathbb{R}^3, ||\boldsymbol{z}|| = 1$, behaves in the following way:

• Either, it increases from a finite value μ_Δ^j to $+\infty$,

• Or, it increases from $-\infty$ to $+\infty$.

Hence, as before, in each interval $]\sqrt{\lambda^j}, \sqrt{\lambda^{j+1}}[$, it may exist a value ω_Δ^j such that

the largest eigenvalue of $A^*(\omega)$ takes negative values in each interval $]\sqrt{\lambda^j}, \omega_\Delta^j[$ with possibly $\omega_\Delta^j = \sqrt{\lambda^j}$; in the latter case, the largest eigenvalue is positive in the whole domain.

5.2 Strong and weak band gaps

With the notations introduced in the previous section, we call *strong band gap* the interval $]\sqrt{\lambda^j}, \omega_\Delta^j[$ and *weak band gap* the interval $]\omega_\Delta^j, \omega_\nabla^j[$, with possibly $\omega_\Delta^j = \sqrt{\lambda^j}$ or $\omega_\nabla^j = \sqrt{\lambda^{j+1}}$. This means that, in a strong band gap, matrix A^* is negative definite and there is no propagation in *any direction*; in a weak band gap, matrix A^* is neither positive nor negative, there is propagation in *at least one direction* corresponding to its positive eigenvalue. Finally, in the interval $]\omega_\nabla^j, \sqrt{\lambda^{j+1}}[$ matrix A^* is positive definite, there is propagation in *all directions*. Thus, in each interval $]\sqrt{\lambda^j}, \sqrt{\lambda^{j+1}}[$, four situations may happen: either the whole interval is formed by only one weak band gap, or by a weak band gap $]\sqrt{\lambda^j}, \omega_\nabla^j[$ followed by a propagation zone $]\omega_\nabla^j, \sqrt{\lambda^{j+1}}[$, or by a strong band gap $]\sqrt{\lambda^j}, \omega_\Delta^j[$ followed by a weak band gap $]\omega_\Delta^j, \sqrt{\lambda^{j+1}}[$, or for the last configuration, by a strong band gap $]\sqrt{\lambda^j}, \omega_\Delta^j[$ followed by a weak band gap $]\omega_\Delta^j, \omega_\nabla^j[$ and next by a propagation zone $]\omega_\nabla^j, \sqrt{\lambda^{j+1}}[$.

Let us insist on the introduction of these definitions which are justified by their importance on the applications (such as for example noise suppression or reduction in *one* or *all* directions).

6 Proof of the existence and convergence Theorems.

The convergence relies partly on Bouchitté and Feldbacq's results established in the Helmoltz diffusion case [4]. We generalize their approach to the framework of linearized elasticity. The proof of the convergence Theorem is broken into 7 steps. In Step 1 we assume that the sequence of solutions $\{\boldsymbol{u}^\varepsilon\}_\varepsilon$ is uniformly bounded in $\boldsymbol{L}^2(\Omega)$. This yields, in Step 2, to the existence of two limit fields $\boldsymbol{u}^1, \boldsymbol{u}^2$, and of a corrector $\overline{\boldsymbol{u}}$ which are coupled solutions to the limit problem. In Step 3 we solve this limit problem, so that the limit field $\boldsymbol{u}^1$ is solution to a wave propagation equation and we identify $\boldsymbol{u}^2$ and $\overline{\boldsymbol{u}}$ as solution to variational problems. In Step 4, we establish the existence of a unique solution for the limit problem (2). In Step 5 we show the strong convergence of the sequence $\{\mathcal{T}^\varepsilon \boldsymbol{u}^\varepsilon\}_\varepsilon$, and finally in Step 6 we show by contradiction, that the *a priori* bound is satisfied, this conclude the proof. Finally, in Step 7, we prove the existence of a unique solution for problem (1) for small enough values of ε.

Step 1. We begin by an *a priori* assumption. Let us suppose that the sequence $\{\boldsymbol{u}^\varepsilon\}_\varepsilon$ is bounded uniformly in ε, i.e., there exists a constant $C > 0$ such that for all $\varepsilon > 0$,

$$||\boldsymbol{u}^\varepsilon||_{\boldsymbol{L}^2(\Omega)} \leq C.$$

Hence, by taking in the stationary problem (1), the test function $\Phi = \boldsymbol{u}^\varepsilon$, we get:

$$\int_{\Omega_1^\varepsilon} c^\varepsilon_{mnkl} e_{kl}(\boldsymbol{u}^\varepsilon) e_{mn}(\boldsymbol{u}^\varepsilon) + \int_{\Omega_2^\varepsilon} c^\varepsilon_{mnkl} e_{kl}(\boldsymbol{u}^\varepsilon) e_{mn}(\boldsymbol{u}^\varepsilon) = \omega^2 \int_\Omega r^\varepsilon |\boldsymbol{u}^\varepsilon|^2 + \int_\Omega \boldsymbol{f} \cdot \boldsymbol{u}^\varepsilon,$$

and the scaling (given in Section 3.2) and coercivity condition (given in Section 2) on the elasticity tensor c^ε yields:

$$\alpha\Big(\int_{\Omega_1^\varepsilon} e_{kl}(\boldsymbol{u}^\varepsilon) e_{kl}(\boldsymbol{u}^\varepsilon) + \varepsilon^2 \int_{\Omega_2^\varepsilon} e_{kl}(\boldsymbol{u}^\varepsilon) e_{kl}(\boldsymbol{u}^\varepsilon) \Big) \leq \omega^2 \rho_2 \int_\Omega |\boldsymbol{u}^\varepsilon|^2 + \int_\Omega \boldsymbol{f} \cdot \boldsymbol{u}^\varepsilon.$$

Therefore, the *a priori* assumption yield the following majoration:

$$||e_{kl}(\boldsymbol{u}^\varepsilon)||_{\boldsymbol{L}^2(\Omega_1^\varepsilon)} + ||\varepsilon e_{kl}(\boldsymbol{u}^\varepsilon)||_{\boldsymbol{L}^2(\Omega_2^\varepsilon)} \leq C, \quad 1 \leq k, l \leq 3, \tag{4}$$

where C is a constant independent of ε.

Step 2. Convergence of the unfolded sequences
For all open set $\mathcal{O} \subset \mathbb{R}^3$ let us introduce the elasticity semi-norm (equivalent to the $\boldsymbol{H}_0^1(\mathcal{O})$ norm):

$$|\boldsymbol{v}|_{\mathcal{E},\mathcal{O}} = \sum_{i,j} ||e_{ij}(\boldsymbol{v})||_{\boldsymbol{L}^2(\mathcal{O})}.$$

Since we have the inclusion $\overline{Y}_2 \subset Y_1$ and the boundary of Y_2 is Lipschitz-continuous, there exists a linear and continuous extension operator $\mathcal{P} : H^1(Y_1) \longrightarrow H^1(Y)$.

Lemma 1. Extension of a bounded vector field
Let $\boldsymbol{v} \in \boldsymbol{H}^1(\Omega_1^\varepsilon)$, there exists an extension $\overline{\boldsymbol{v}} \in \boldsymbol{H}^1(\Omega)$ that satisfies the bound:

$$|\overline{\boldsymbol{v}}|_{\mathcal{E},\Omega} \leq C |\boldsymbol{v}|_{\mathcal{E},\Omega_1^\varepsilon},$$

with C independent of ε.
Proof. First we consider a displacement field $\boldsymbol{v} \in \boldsymbol{H}^1(Y_1)$. There exists a rigid displacement $\boldsymbol{r}$ such that:

$$||\boldsymbol{v} - \boldsymbol{r}||_{\boldsymbol{H}^1(Y_1)} \leq C |\boldsymbol{v}|_{\mathcal{E},Y_1}.$$

Hence we can define the extension $\overline{\boldsymbol{v}}$ by:

$$\overline{\boldsymbol{v}} = \begin{cases} (\boldsymbol{v}-\boldsymbol{r})+\boldsymbol{r} & \text{in} \quad Y_1, \\ \mathcal{P}(\boldsymbol{v}-\boldsymbol{r})+\boldsymbol{r} & \text{in} \quad Y_2, \end{cases}$$

and obviously we get

$$|\overline{\boldsymbol{v}}|_{\mathcal{E},Y} \leq C|\boldsymbol{v}|_{\mathcal{E},Y_1}.$$

Next we consider a displacement field $\boldsymbol{v} \in \boldsymbol{H}^1(\Omega_1^\varepsilon)$. With the same extension operator we can define the extension $\overline{\boldsymbol{v}} \in \boldsymbol{H}^1(\Omega)$ and get the majoration $|\overline{\boldsymbol{v}}|_{\mathcal{E},\Omega} \leq C|\boldsymbol{v}|_{\mathcal{E},\Omega_1^\varepsilon}$ with C independent of ε.

Corollary of Lemma 1. Decomposition of the displacement field $\boldsymbol{u}^\varepsilon$
There exists two displacement fields $\boldsymbol{u}^{\varepsilon,1}$ and $\boldsymbol{u}^{\varepsilon,2}$ such that the solution $\boldsymbol{u}^\varepsilon$ of problem (1) can be decomposed as:

$$\boldsymbol{u}^\varepsilon = \boldsymbol{u}^{\varepsilon,1} + \boldsymbol{u}^{\varepsilon,2}.$$

(i) The displacement field $\boldsymbol{u}^{\varepsilon,1} \in \boldsymbol{H}_0^1(\Omega)$ coincides with $\boldsymbol{u}^\varepsilon$ in Ω_1^ε and satisfies the bound:

$$|\boldsymbol{u}^{\varepsilon,1}|_{\mathcal{E},\Omega} \leq C|\boldsymbol{u}^\varepsilon|_{\mathcal{E},\Omega_1^\varepsilon}$$

with a constant C independent of ε.
(ii) The displacement field $\boldsymbol{u}^{\varepsilon,2} \in \boldsymbol{H}_0^1(\Omega)$ vanishes in Ω_1^ε.
(iii) Moreover, we have the bounds $|\boldsymbol{u}^{\varepsilon,1}|_{\mathcal{E},\Omega} \leq C, \quad |\boldsymbol{u}^{\varepsilon,2}|_{\mathcal{E},\Omega} \leq \dfrac{C}{\varepsilon}$, which yield

$$||\boldsymbol{u}^{\varepsilon,1}||_{\boldsymbol{H}^1(\Omega)} \leq C, \quad ||\boldsymbol{u}^{\varepsilon,2}||_{\boldsymbol{L}^2(\Omega)} \leq C. \tag{5}$$

Proof. We denote by $\boldsymbol{v}^\varepsilon$ the restriction of $\boldsymbol{u}^\varepsilon$ to Ω_1^ε. By Lemma 1, let $\boldsymbol{u}^{\varepsilon,1}$ be the extension of $\boldsymbol{v}^\varepsilon$ to Ω, $\boldsymbol{u}^{\varepsilon,1} = \overline{\boldsymbol{v}^\varepsilon}$, and we get the majoration of step (i). Since $\boldsymbol{u}^{\varepsilon,1} = \boldsymbol{u}^\varepsilon$ in Ω_1^ε we get step (ii). Step (iii) is a consequence of bounds (4).

The homogenization method presented in section 3 and majorations (4) and (5) yield the following convergence result.
Lemma 2.
(i) There exists two limit vector fields $\boldsymbol{u}^1, \boldsymbol{u}^2$ and a corrector $\overline{\boldsymbol{u}}$,

$$\boldsymbol{u}^1 \in \boldsymbol{H}_0^1(\Omega), \boldsymbol{u}^2 \in \boldsymbol{L}^2(\Omega; \boldsymbol{H}_0^1(Y_2)), \overline{\boldsymbol{u}} \in \boldsymbol{L}^2(\Omega; \boldsymbol{H}_{per}^1(Y)), \int_Y \overline{\boldsymbol{u}} = \boldsymbol{0}$$

such that, up to subsequences still denoted with the same indices, we have the convergences:

$$\begin{cases} \mathcal{T}^\varepsilon(\boldsymbol{u}^{1,\varepsilon}) & \rightharpoonup \boldsymbol{u}^1 & \text{weakly in } \boldsymbol{L}^2(\Omega\times Y), \\ \mathcal{T}^\varepsilon(e_{kl}(\boldsymbol{u}^{1,\varepsilon})) & \rightharpoonup e_{kl,x}(\boldsymbol{u}^1)+e_{kl,y}(\overline{\boldsymbol{u}}) & \text{weakly in } \boldsymbol{L}^2(\Omega\times Y), \\ \mathcal{T}^\varepsilon(\boldsymbol{u}^{\varepsilon,2}) & \rightharpoonup \boldsymbol{u}^2 & \text{weakly in } \boldsymbol{L}^2(\Omega\times Y_2), \\ \varepsilon\mathcal{T}^\varepsilon(e_{kl}(\boldsymbol{u}^{\varepsilon,2})) & \rightharpoonup e_{kl,y}(\boldsymbol{u}^2) & \text{weakly in } \boldsymbol{L}^2(\Omega\times Y_2). \end{cases}$$

(ii) *The three fields* $(\boldsymbol{u}^1,\boldsymbol{u}^2,\overline{\boldsymbol{u}})$ *solve the following three coupled variational problems:*

$$\begin{cases} \displaystyle\int_{Y_1} c_{1,mnkl}(y)\Big(e_{kl,x}(\boldsymbol{u}^1(x))+e_{kl,y}(\overline{\boldsymbol{u}}(x,y))\Big)e_{mn}(\overline{\Phi}(y))dy=0 \quad \text{for all} \quad \overline{\Phi}\in\boldsymbol{H}^1_{per}(Y_1), \\ \omega^2\displaystyle\int_{Y_2} r_2(y)(\boldsymbol{u}^1(x)+\boldsymbol{u}^2(x,y))\cdot\overline{\Psi}(y)dy-\int_{Y_2} c_{2,mnkl}(y)e_{kl,y}(\boldsymbol{u}^2(x,y))e_{mn,y}(\overline{\Psi}(y))dy \\ \qquad\qquad =-\boldsymbol{f}(x)\cdot\displaystyle\int_{Y_2}\overline{\Psi}(y)dy \quad \text{for all } \overline{\Psi}\in\boldsymbol{H}^1_0(Y_2), \\ \omega^2\displaystyle\int_\Omega \boldsymbol{u}^1(x)\cdot\Phi(x)(\int_Y r(y)dy)dx+\omega^2\int_\Omega\Phi(x)\cdot(\int_{Y_2} r_2(y)\boldsymbol{u}^2(x,y)dy)dx \\ \qquad\qquad -\displaystyle\int_{\Omega\times Y_1} c_{1,mnkl}(y)\Big(e_{kl,x}(\boldsymbol{u}^1(x))+e_{kl,y}(\overline{\boldsymbol{u}}(x,y))\Big)e_{mn}(\Phi(x))dx \\ \qquad\qquad =-\displaystyle\int_\Omega \boldsymbol{f}(x)\cdot\Phi(x)dx \quad \text{for all} \quad \Phi\in\boldsymbol{H}^1_0(\Omega). \end{cases}$$

Proof. Weak convergences (i) are obtained by using the bounds (4), (5) and the properties of the unfolding operator. The limit problems of part (ii) are obtained with appropriate test-functions in problem (1). More precisely:
-For the first problem we choose test-functions of the form: $\varepsilon w(x)\Phi(\{\frac{x}{\varepsilon}\}), x\in\Omega$, with $w\in\mathcal{D}(\Omega),\Phi\in\boldsymbol{H}^1_{per}(Y)$.
-For the second problem we choose test-functions of the form:

$$\begin{cases} w(x)\Psi(\{\frac{x}{\varepsilon}\}) & x\in\Omega_2^\varepsilon, \\ 0 & x\in\Omega_1^\varepsilon. \end{cases}$$

with $w\in\mathcal{D}(\Omega),\Psi\in\boldsymbol{H}^1_0(Y_2)$.
-For the last problem we choose test-functions of the form: $\Phi\in\boldsymbol{H}^1_0(\Omega)$.

Step 3. In this step we solve, successively, each limit variational problem.
• *First we solve the problem posed in Y_1 to compute the corrector $\overline{\boldsymbol{u}}$.*

$$\int_{Y_1} c_{1,mnkl}(y)\Big(e_{kl,x}(\boldsymbol{u}^1)+e_{kl,y}(\overline{\boldsymbol{u}})\Big)e_{mn}(\overline{\Phi})=0 \quad \text{for all} \quad \overline{\Phi}\in \boldsymbol{H}^1_{per}(Y_1).$$

The corrector $\overline{\boldsymbol{u}}$ is expressed as the linear combination $\overline{\boldsymbol{u}}(x,y)=e_{mn,x}(\boldsymbol{u}^1(x))\boldsymbol{z}_{mn}(y)$ where the basis functions $\boldsymbol{z}_{mn}\in \boldsymbol{H}^1_{per}(Y_1)$ are solutions to the variational problems (by symmetry, there exists only 6 different problems in three-dimensional elasticity and 3 different problems in two-dimensional elasticity):

$$\int_{Y_1} c_{1,ijkl}\Big(e_{kl,y}(\boldsymbol{z}_{mn})+\delta^{kl}_{mn}\Big)e_{ij,y}(\overline{\Phi}))dy=0 \quad \text{for all} \quad \overline{\Phi}\in \boldsymbol{H}^1_{per}(Y_1),$$

hence, we get the homogeneous (independent of x) tensor c^*:

$$c^*_{ijkl}=\int_{Y_1} c_{1,ijmn}\Big(e_{mn,y}(\boldsymbol{z}_{kl})+\delta^{kl}_{mn}\Big)dy, \tag{6}$$

and δ^{kl}_{mn} is the Kronecker symbol $\delta^{kl}_{mn}=0$ for $m\neq k$ or $n\neq l,$ and $\delta^{mn}_{mn}=1$. It is easy to show that tensor c^* has the same properties of symmetry and coercivity of the initial one c^ε.
Let us remark that c^* is independent of ω and only depends upon the value of the elasticity tensor c_1 within the matrix and the shape of the matrix, more precisely the shape of the elementary inclusion Y_1, the same result would have been obtained with a perforated domain, Y_2 being the hole. It is important also to note that the corrector $\overline{\boldsymbol{u}}$ is not determined in Y_2.
• *Next we solve the problem posed in Y_2, this allows the computation of $\boldsymbol{u}^2$*:

$$\begin{aligned}\omega^2\int_{Y_2} r_2(y)\boldsymbol{u}^2\cdot\overline{\Psi}-\int_{Y_2} c_{2,mnkl}(y)e_{kl,y}(\boldsymbol{u}^2)e_{mn,y}(\overline{\Psi})\\ =-\omega^2\boldsymbol{u}^1\cdot\int_{Y_2} r_2(y)\overline{\Psi}-\boldsymbol{f}\cdot\int_{Y_2}\overline{\Psi}\quad \text{for all } \overline{\Psi}\in \boldsymbol{H}^1_0(Y_2).\end{aligned}$$

Let us examine the spectral properties of the previous problem in $\boldsymbol{u}^2$. We note $\{\varphi^j,\lambda^j\}_{j\geq 1}$ the eigenelements associated to the elasticity operator. The positivity of r_2 and the coercivity of tensor c_2 imply that the eigenvalues $\{\lambda^j\}_{j\geq 1}$ are real and positive, let us range them in ascending order, $0\leq\cdot\cdot\leq\lambda^j\leq\lambda^{j+1}\leq\cdot\cdot$

$$\begin{cases}\displaystyle\int_{Y_2} c_{2,mnkl}(y)e_{kl,y}(\varphi^j)e_{mn,y}(\overline{\Psi})=\lambda^j\int_{Y_2} r_2(y)\varphi^j\cdot\overline{\Psi}\quad \text{for all } \overline{\Psi}\in \boldsymbol{H}^1_0(Y_2),\\ \text{without summation on } j,\\ \text{and with the orthogonality condition}\quad \displaystyle\int_{Y_2} r_2(y)\varphi^p\cdot\varphi^q=\delta^q_p,.\end{cases} \tag{7}$$

We decompose $\boldsymbol{u}^2$ in the basis of the eigenvectors $\{\phi^j\}_{j\geq 1}$. Hence for all frequencies *different from the resonance* $\omega^2 \neq \lambda^j, j \in J$ with

$$J = \{j \geq 1, \int_{Y_2} r_2(y)\varphi^j(y)dy \neq 0\}, \tag{8}$$

the displacement field $\boldsymbol{u}^2$ can be explicitly given in terms of $\boldsymbol{u}^1$ by the series:

$$\boldsymbol{u}^2(x,y) = \sum_{j\geq 1} \frac{-\omega^2 \boldsymbol{u}^1(x)\cdot \int_{Y_2} r_2(y)\varphi^j(y)}{\omega^2-\lambda^j}\varphi^j(y) - \frac{\boldsymbol{f}(x)\cdot \int_{Y_2}\varphi^j(y)}{\omega^2-\lambda^j}\varphi^j(y).$$

• *Finally we solve the problem posed in* Ω *to get the limit elastic field* $\boldsymbol{u}^1$:

$$\begin{aligned}\omega^2 \int_\Omega \boldsymbol{u}^1\cdot\Phi \int_Y r(y) + \omega^2 \int_\Omega \Phi\cdot\int_{Y_2} r_2(y)\boldsymbol{u}^2(x,y) - \int_\Omega c^*_{mnkl}e_{kl}(\boldsymbol{u}^1)e_{ij}(\Phi)\\ = -\int_\Omega \boldsymbol{f}\cdot\Phi \quad \text{for all} \quad \Phi \in \boldsymbol{H}^1_0(\Omega).\end{aligned}$$

We replace $\boldsymbol{u}^2$ by the expression obtained previously, this yields

$$\int_{Y_2} r_2(y)\boldsymbol{u}^2(x,y)\cdot\Phi(x) = -\omega^2 A(\omega)\boldsymbol{u}^1(x)\cdot\Phi(x) - B(\omega)\boldsymbol{f}(x)\cdot\Phi(x),$$

where matrices $A = (A_{qp})$ and $B = (B_{qp})$ (of order 3) are given by:

$$\begin{cases} A_{qp}(\omega) = \displaystyle\sum_{j\in J} \frac{\int_{Y_2} r_2(y)\varphi^j_p(y)\int_{Y_2} r_2(y)\varphi^j_q(y)}{\omega^2-\lambda^j}, \\ \\ B_{qp}(\omega) = \displaystyle\sum_{j\in J} \frac{\int_{Y_2} \varphi^j_p(y)\int_{Y_2} r_2(y)\varphi^j_q(y)}{\omega^2-\lambda^j}, \end{cases}$$

and a straightforward computation leads to the limit problem (2) with

$$\begin{cases} A^*(\omega) = -\omega^2 A(\omega) + r^* I, \quad r^* = \int_{Y_1} r_1(y)dy + \int_{Y_2} r_2(y)dy, \\ B^*(\omega) = -\omega^2 B(\omega) + I. \end{cases} \tag{9}$$

Step 4. As stated in section 5.2, for certain types of data (geometry of Y_2 and values of c^ε and r^ε) it may happen that there is *no* zone of wave propagation, this is the case when for all $j \in J$, $\omega^j_\nabla = \sqrt{\lambda^{j+1}}$. Therefore to establish the existence of

the solution to the limit problem, we *assume* that there exists a set, still denoted J, such that $\omega_\nabla^j < \sqrt{\lambda^{j+1}}$ for all $j \in J$. With this assumption we have the following existence lemma.

Lemma 3. *There exists a non empty, open set $W \subset \mathbb{R}^+$ such that for all frequencies $\omega \in W$ the limit problem (2) has a unique solution.*

Proof. Matrix $A^*(\omega)$ is positive definite for all $\omega \in]\omega_\nabla^j, \sqrt{\lambda^{j+1}}[, j \in J$. In each interval of this type there exists a countable set of resonance frequencies $\{\omega_k^j\}_{k\in K^j}$ such that for all $\omega \neq \omega_k^j$ the following problem has a unique vanishing solution:

$$\omega^2 \int_\Omega A^*(\omega)\boldsymbol{v}(x)\cdot\Phi(x)dx - \int_\Omega c^*_{mnkl}e_{kl}(\boldsymbol{v}(x))e_{mn}(\Phi(x))dx = 0 \quad \forall\Phi \in H_0^1(\Omega).$$

Let $W = \{\omega \in]\omega_\nabla^j, \sqrt{\lambda^{j+1}}[, \omega \neq \omega_k^j, k \in K^j, j \in J\}$. Hence, by Fredholm alternative, problem (2) has a unique solution for all $\omega \in W$.

An easy way to assure the existence of such a set W is to increase the mass density r_1 which implies the existence of a non empty domain of frequencies where A^* is definite positive.

Step 5. In this section we establish *the strong convergence* of the sequence $\{\mathcal{T}^\varepsilon(\boldsymbol{u}^\varepsilon)\}_\varepsilon$ in the space $\boldsymbol{L}^2(\Omega\times Y)$.

According to Corollary of Lemma 1 and Lemma 2, up to subsequences still denoted with the same indices, we have the convergence:

$$\left\{\begin{array}{lcll} \boldsymbol{u}^{\varepsilon,1} & \longrightarrow & \boldsymbol{u}^1 & \text{strongly in } \boldsymbol{L}^2(\Omega), \\ \mathcal{T}^\varepsilon(\boldsymbol{u}^{\varepsilon,2}) & \rightharpoonup & \boldsymbol{u}^2 & \text{weakly in } \boldsymbol{L}^2(\Omega\times Y). \end{array}\right.$$

Using the decomposition $\boldsymbol{u}^\varepsilon = \boldsymbol{u}^{\varepsilon,1} + \boldsymbol{u}^{\varepsilon,2}$ we rewrite problem (1) in the following way:

$$\begin{aligned} &\omega^2 \int_{\Omega_2^\varepsilon} r^\varepsilon \boldsymbol{u}^{\varepsilon,2}\cdot\Phi - \varepsilon^2 \int_{\Omega_2^\varepsilon} c^\varepsilon_{mnkl}e_{kl}(\boldsymbol{u}^{\varepsilon,2})e_{mn}(\Phi) \\ &= \varepsilon^2 \int_{\Omega_2^\varepsilon} c^\varepsilon_{mnkl}e_{kl}(\boldsymbol{u}^{\varepsilon,1})e_{mn}(\Phi) - \int_{\Omega_2^\varepsilon}(\boldsymbol{f} + \omega^2 r^\varepsilon \boldsymbol{u}^{\varepsilon,1})\cdot\Phi \quad \forall\Phi \in \boldsymbol{H}_0^1(\Omega_2^\varepsilon). \end{aligned}$$

Since the unit cells are disjointed, the previous system reduces to a problem posed in Y_2: For almost all $x \in \Omega$ find $\mathcal{T}^\varepsilon(\boldsymbol{u}^{\varepsilon,2})(x,y) \in \boldsymbol{H}_0^1(Y_2)$ such that:

$$\begin{aligned} &\omega^2 \int_{Y_2} r_2 \mathcal{T}^\varepsilon(\boldsymbol{u}^{\varepsilon,2})(x,.)\cdot\Phi - \int_{Y_2} c_{2,mnkl}e_{kl,y}(\mathcal{T}^\varepsilon(\boldsymbol{u}^{\varepsilon,2})(x,.))e_{mn,y}(\Phi) \\ &= \varepsilon \int_{Y_2} c_{2,mnkl}e_{kl}(\mathcal{T}^\varepsilon(\boldsymbol{u}^{\varepsilon,1})(x,.))e_{mn,y}(\Phi) - \int_{Y_2}\mathcal{T}^\varepsilon(\boldsymbol{f} + \omega^2 r_2 \boldsymbol{u}^{\varepsilon,1})(x,.)\cdot\Phi \\ &\qquad \forall\Phi \in \boldsymbol{H}_0^1(Y_2). \end{aligned}$$

We make use of the eigen basis $(\varphi^j)_{j\geq 1}$ introduced in (7) to express the solution $\mathcal{T}^\varepsilon(\boldsymbol{u}^{\varepsilon,2})$ as:

$$\begin{aligned}\mathcal{T}^\varepsilon(\boldsymbol{u}^{\varepsilon,2})(x,y) = & \sum_{j\geq 1} \frac{\varepsilon \int_{Y_2} c_{2,mnkl} e_{kl}(\mathcal{T}^\varepsilon(\boldsymbol{u}^{\varepsilon,1})(x,s)) e_{mn,y}(\varphi^j(s))ds}{\omega^2-\lambda^j}\varphi^j(y) \\ & -\sum_{j\geq 1} \frac{\int_{Y_2} \mathcal{T}^\varepsilon(\boldsymbol{f}+\omega^2 r_2 \boldsymbol{u}^{\varepsilon,1})(x,s)\cdot\varphi^j(s)ds}{\omega^2-\lambda^j}\varphi^j(y).\end{aligned}$$

And by linearity of the unfolding operator $\mathcal{T}^\varepsilon$ we get

$$\begin{aligned}\mathcal{T}^\varepsilon(\boldsymbol{u}^{\varepsilon,2}) - \boldsymbol{u}^2 = & \sum_{j\geq 1} \frac{\varepsilon \int_{Y_2} c_{2,mnkl} e_{kl}(\mathcal{T}^\varepsilon(\boldsymbol{u}^{\varepsilon,1})(x,s)) e_{mn,y}(\varphi^j(s))ds}{\omega^2-\lambda^j}\varphi^j(y) \\ & -\sum_{j\geq 1} \frac{\int_{Y_2} (\mathcal{T}^\varepsilon(\boldsymbol{f})-\boldsymbol{f})(x,s)\cdot\varphi^j(s)ds}{\omega^2-\lambda^j}\varphi^j(y) \\ & -\sum_{j\geq 1} \frac{\int_{Y_2} \omega^2 r_2(\mathcal{T}^\varepsilon(\boldsymbol{u}^{\varepsilon,1})-\boldsymbol{u}^1)(x,s)\cdot\varphi^j(s)ds}{\omega^2-\lambda^j}\varphi^j(y).\end{aligned}$$

Hence, from the convergence

$$\left\{\begin{array}{lll} \mathcal{T}^\varepsilon(\boldsymbol{f}) & \longrightarrow \boldsymbol{f} & \text{strongly in } \boldsymbol{L}^2(\Omega\times Y), \\ \mathcal{T}^\varepsilon(\boldsymbol{u}^{\varepsilon,1}) & \longrightarrow \boldsymbol{u}^1 & \text{strongly in } \boldsymbol{L}^2(\Omega\times Y), \end{array}\right.$$

we get the strong convergence,

$$\left\{\begin{array}{lll} \mathcal{T}^\varepsilon(\boldsymbol{u}^{\varepsilon,2}) & \longrightarrow \boldsymbol{u}^2 & \text{strongly in } \boldsymbol{L}^2(\Omega\times Y), \\ \mathcal{T}^\varepsilon(\boldsymbol{u}^{\varepsilon}) & \longrightarrow \boldsymbol{u}^1+\boldsymbol{u}^2 & \text{strongly in } \boldsymbol{L}^2(\Omega\times Y), \end{array}\right.$$

which implies

$$\int_\Omega |\boldsymbol{u}^\varepsilon(x)|^2 dx \longrightarrow \int_{\Omega\times Y} |\boldsymbol{u}^1(x)+\boldsymbol{u}^2(x,y)|^2 dxdy.$$

Step 6. We are now in a position to justify the *a priori* boundedness assumption of Step 1. Let us assume, by contradiction, that $||\boldsymbol{u}^\varepsilon||_{L^2(\Omega)} \longrightarrow \infty$ and let us consider the displacement field $\tilde{\boldsymbol{u}^\varepsilon} = \dfrac{\boldsymbol{u}^\varepsilon}{||\boldsymbol{u}^\varepsilon||_{\boldsymbol{L}^2(\Omega)}}$. This field is solution to a problem

similar to the initial one (1) but where the right-hand side $\boldsymbol{f}$ has been replaced by $\tilde{\boldsymbol{f}}^{\varepsilon} = \dfrac{\boldsymbol{f}}{||\boldsymbol{u}^{\varepsilon}||_{\boldsymbol{L}^2(\Omega)}}$, $||\tilde{\boldsymbol{f}}^{\varepsilon}||_{L^2(\Omega)} \longrightarrow \mathbf{0}$. The sequence $\{||\tilde{\boldsymbol{u}^{\varepsilon}}||_{\boldsymbol{L}^2(\Omega)}\}_{\varepsilon}$ is uniformly bounded, the convergence Theorem 2 can be applied for all admissible frequencies, $\omega \in W$, to show that the sequence $\{\mathcal{T}^{\varepsilon}(\tilde{\boldsymbol{u}^{\varepsilon}})\}_{\varepsilon}$ strongly converges to a vanishing displacement field, this states the contradiction.

Step 7. Finally we prove, for ε small enough, the Existence Theorem 1 for the initial problem (1). Let us proceed by contradiction. We consider a vanishing applied force $\boldsymbol{f} = \mathbf{0}$ and a sequence of strictly positive numbers $\{\varepsilon_p\}_{p\in\mathbb{N}^*}$ converging to zero and such that, for all $p \in \mathbb{N}^*$, there exists a displacement field $\boldsymbol{u}^{\varepsilon_p} \in \boldsymbol{H}_0^1(\Omega)$, solution to problem (1) which satisfies $||\boldsymbol{u}^{\varepsilon_p}||_{\boldsymbol{L}^2(\Omega)} = 1$, thus:

$$\omega^2 \int_{\Omega} r^{\varepsilon_p} \boldsymbol{u}^{\varepsilon_p} \cdot \Phi - \int_{\Omega} c_{mnkl}^{\varepsilon_p} e_{kl}(\boldsymbol{u}^{\varepsilon_p}) e_{mn}(\Phi) = 0 \quad \forall \Phi \in \boldsymbol{H}_0^1(\Omega).$$

From the strong convergence of Step 5 we get $\displaystyle\int_{\Omega} |\boldsymbol{u}^{\varepsilon_p}|^2 \longrightarrow \int_{\Omega\times Y} |\boldsymbol{u}^1 + \boldsymbol{u}^2|^2$. By assumption (ii), for all $\omega \in W$, we have $\boldsymbol{u}^1$ as the unique (vanishing) solution to the limit problem:

$$\omega^2 \int_{\Omega} A^*(\omega)\boldsymbol{u}^1(x)\cdot\Phi(x)dx - \int_{\Omega} c^*_{mnkl} e_{kl}(\boldsymbol{u}^1(x)) e_{mn}(\Phi(x))dx = 0 \quad \forall \Phi \in \boldsymbol{H}_0^1(\Omega)$$

and next the computation gives $\boldsymbol{u}^2 = \mathbf{0}$ which implies a contradiction.

7 Numerical illustration in the two-dimensional case

In this section we provide some numerical simulations to illustrate the *acoustic band gaps* determined by the eigenvalues of $A^*(\omega)$ and the effect of changing the parameters of the model, in particular we investigate the influence of the *average material mass density* and of the *geometry of the microstructure*.

The theoretical results obtained in the previous sections were given in the framework of three-dimensional elasticity, of course they apply as well in the two-dimensional case of in-plane vibrations. Therefore, in order to reduce the computational effort (since in this case we have the explicit formulae of both eigenvalues of A^* at hand, i.e., without any further computing) we restrict our work to the two-dimensional case which exhibits the most important characteristics of the band gaps structure.

The numerical identification of the band gaps is done through the following steps:

1. Computation by the finite element method of the approximate value $(\tilde{\lambda}^j, \tilde{\varphi}^j), j \in \mathbb{N}$ of the eigenelements (λ^j, φ^j) of the elasticity problem (7) posed over Y_2.

2. Determination of the reduced index set $\tilde{J}$ by eliminating the eigenvalues that do not contribute to the expression of A^*, thanks to the introduction of a threshold τ,
$$\tilde{J} = \{j \geq 1, | \int_{Y_2} r_2(y)\tilde{\varphi}^j(y)dy| > \tau\}.$$

3. In each interval $]\sqrt{\tilde{\lambda}^j}, \sqrt{\tilde{\lambda}^{j+1}}[$, $j \in \tilde{J}$, and for selected frequencies ω,
• Compute the entries of matrix $\tilde{A}^*(\omega)$ by replacing the infinite sum over the index set J, see (8) by the ***finite sum*** over $\tilde{J}$,
$$\tilde{A}^*(\omega) = \sum_{j \in \tilde{J}} \tilde{A}^{*,j}(\omega) + r^* I.$$
• Compute *explicitly* the largest and the smallest eigenvalues denoted by $\tilde{\mu}_\Delta(\omega)$ and $\tilde{\mu}_\nabla(\omega)$ of matrix $\tilde{A}^*(\omega)$.
• Localize numerically the frequencies denoted by $\tilde{\omega}^j_\nabla$ (respectively $\tilde{\omega}^j_\Delta$), for which the smallest eigenvalue (respectively the largest eigenvalue) of $\tilde{A}^*(\omega)$ vanishes. Hence the *strong* and *weak* band gaps and the *wave propagation* zone can easily be identified.

The numerical examples presented below have been obtained by using an in-house software based on the MATLAB computational tools. For analysis of the eigenvalue elasticity problem (7) defined in domain Y_2 we computed the approximation of the displacement eigenfunctions with linear finite elements on triangular meshes.

7.1 Numerical simulation of strong and weak band gaps

In Figure 1 we display the successive resonance frequencies $\sqrt{\tilde{\lambda}^j}, j \in \tilde{J}$, for elliptic inclusions. Each frequency band $]\sqrt{\tilde{\lambda}^j}, \sqrt{\tilde{\lambda}^{j+1}}[$ is decomposed into one or two zones with no wave propagation (the strong and weak zones) followed by a wave propagation zone. In a weak band, the largest eigenvalue $\tilde{\mu}_\Delta$ of $\tilde{A}^*$ is positive and the other one $\tilde{\mu}_\nabla$ is negative, there is propagation only in the direction of the eigenvector ψ_Δ associated to $\tilde{\mu}_\Delta$. This direction may change when the frequency ω varies. With the same elliptic inclusions as in Figure 1 we display, in Figure 2, the variation (with respect to ω) of the orientation angle of the eigenvector ψ_Δ. For this example, the numerical experiment shows that, within the entire weak band

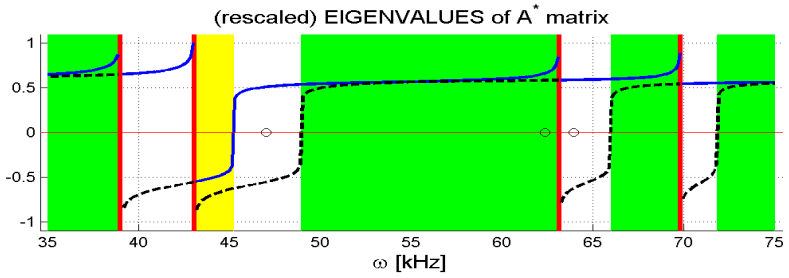

Fig. 1: Band structure for elliptic inclusions. The resonance frequencies $\sqrt{\lambda^j}$ are displayed in red. The largest $\tilde{\mu}_\Delta$ (solid) and smallest $\tilde{\mu}_\nabla$ (dashed) eigenvalues of matrix A^* delineate the wave propagation zones. The bands of unlimited *wave propagation* are displayed in green, the *strong* band gaps are displayed in yellow and the *weak* band gaps are in white. The eigenvalues with a (almost) vanishing contribution in the set $\tilde{J}$ are represented by a circle.

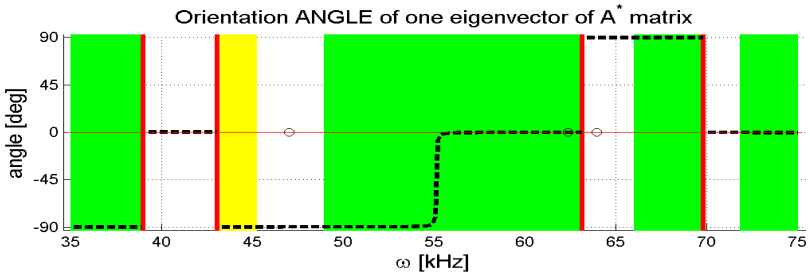

Fig. 2: Band structure for elliptic inclusions. Orientation angle of the eigenvector associated with the largest eigenvalue $\mu_\Delta(\omega)$.

gap, there is *no change* of the direction of ψ_Δ; hence the direction of propagation *remains the same*. It is worth noting that, due to this property, it makes sense for applications to use the *whole* weak gap interval as the propagation zone for suppressing vibrations in the direction orhogonal to ψ_Δ.

However, for more complicated geometries of the inclusions [9], there is a change in the direction of ψ_Δ. In such cases the weak band gaps behave as the strong ones.

7.2 Influence of some microstructural parameters in the band gaps distribution

We illustrate how the acoustic bands depend on some selected features characterizing the microstructure; in particular we study the effects of changing

- the *averaged material density* given by $r^* = (1 - |Y_2|)r_1 + |Y_2|r_2$, when homogeneous materials with mass density r_1 and r_2 are considered respectively in Y_1 Y_2;
- the *shape* of the inclusions, i.e. the shape of Y_2;

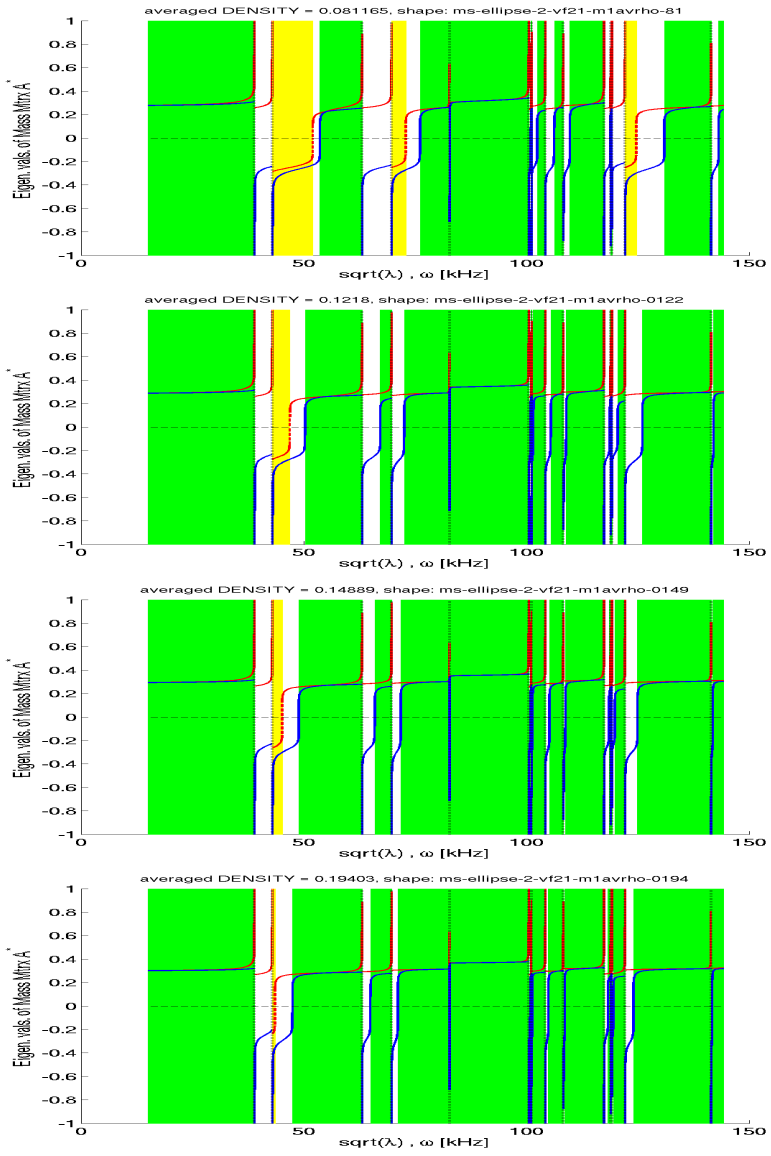

Fig. 3: Influence of the average density variation $r^* = (1 - |Y_2|)qr_1 + |Y_2|r_2$ on an elliptic inclusion Y_2. The value of q is set, from top to bottom, to 25%, 70%, 100% and 150%.

- the *volume fraction* $|Y_2|/|Y|$, i.e. the (relative) size of the inclusions when keeping their shape fixed.

7.2.1 Averaged material density

The influence of the material density in the *inclusion* is rather complex. Obviously a change in density r_2 of the material in Y_2 re-scales the distribution of all resonant frequencies $\sqrt{\tilde{\lambda}^j}, j \in \tilde{J}$ and influences the magnitude of the frequency-dependent part of tensors $A^{*,j}(\omega)$, as well as its isometric part r^*I. By contrast, a change in r_1, i.e. in the density of the *matrix* component, is easy to foresee. It results in a modification of the average density without any impact on the distribution of the resonant frequencies. Nevertheless, such a modification leads to a *shift* in the bounds of both the weak and strong gaps,whereby the quality of the gaps may change also, for example a strong band becoming a weak one or a weak one becoming a full propagation zone. This effect is captured in Figure 3, where the influence of changing the averaged density is tested on an elliptical geometry of Y_2 with $r^* = (1 - |Y_2|)qr_1 + |Y_2|r_2$ the value of q is set to 25%, 70%, 100% and 150%. It can well be observed that *the lighter the matrix is, the larger the band gaps are*; more precisely, a smaller density r_1 results in an increase of the band gap widths.

7.2.2 Shape of the inclusion.

We perform the computation of the band gaps for different shapes of inclusion Y_2 for both symmetric geometries (circles, squares) and non symmetric geometries (ellipses, rectangles); in the latter cases the weak band gaps are distinguishable, in contrast with the case of symmetric inclusions where only strong band gaps (and of course propagating zones) appear.

In Figure 4, the distribution is displayed of the predicted band gaps for the first frequency band. For symmetric micro structures, i.e. those with more than two axes of the symmetry,we obtain $\mu^j_\nabla \equiv \mu^j_\Delta$, which recalls the analogy with the case of diffusion [4].

For highly elongated ellipses the strong gap disappears, see also Figure 4 for the rectangular domains. All the examples displayed here were obtained with a square unit cell Y, however measurements show that other types of lattices, such as hexagonal ones, can be more appropriate to enlarge the band gaps. It would be of interest to investigate such configurations.

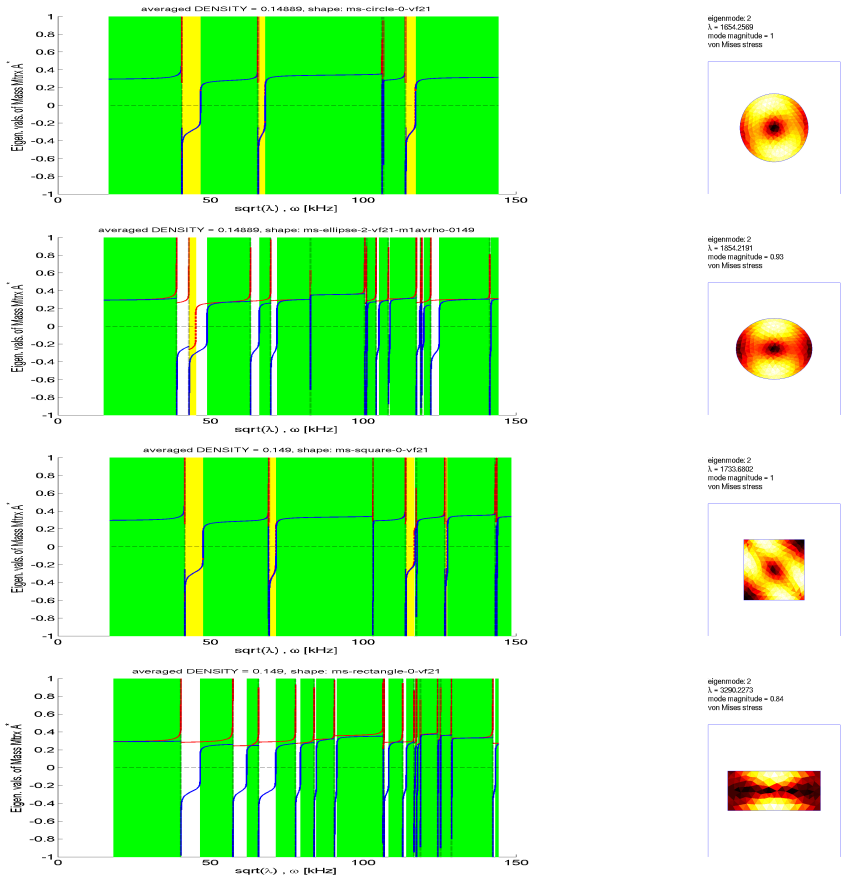

Fig. 4: Influence of the shape of the inclusion Y_2. *Left*: Band gaps distribution. *Right*: The 2nd resonance eigenmode for the corresponding shapes is illustrated in terms of the von Mises stress generated by the eigenfunction φ^2. Note that the 2nd mode φ^2 corresponds to the eigenfrequency $\sqrt{\lambda^2}$ representing the lower bound of the first strong band gap, when it exists.

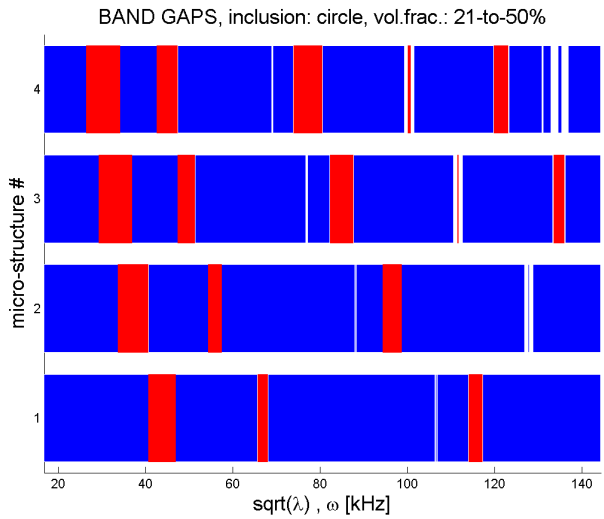

Fig. 5: Influence of the volume fraction $|Y_2|/|Y|$. The microstructures $\#1$, $\#2$, $\#3$, $\#4$ correspond to volume fraction equal to 21, 30, 40 and 50 %.

7.2.3 Volume fraction of the inclusion.

The effect of the "fill-in" coefficient $|Y_2|/|Y|$ of the inclusion can be studied analytically, so that having solved the eigenvalue problem in a domain Y_2 for a fixed volume fraction, the gap distribution can be predicted for other micro structures with re-scaled size of the inclusion. A change in the ratio $|Y_2|/|Y|$ influences the averaged density, but also the magnitudes of the resonance frequencies. When this ratio is increasing, the eigenfrequencies are decreasing and, thereby, the band gaps are "shifted" to lower bands, as illustrated in Figure 5.

As a brief conclusion for this simulation part, we remark that the numerical simulations presented in this section show the sensitivity of the distribution of the wave propagation bands with respect to some physical parameters. The next challenging question to address would be to optimize the design of the micro structures according to some figures of merit (position, reduction, enlargement, shift of the band gaps). The first step of this analysis which is the microstructural sensitivity approach is actually under study [9].

Acknowlegment

This work has been supported by the European project “Smart Systems” HPRN-CT-2002-00284 and by the Chilean projects Fondecyt 1020298 et 7040209 .

References

[1] G. Allaire. *Homogenization and two-scale convergence*, SIAM J. Math. Anal., 23, (6), (1992), 1482-1518.

[2] T. Arbogast, J. Douglas, U. Hornung. *Derivation of the double porosity model of single phase flow via homogenization theory*, SIAM J. Math. Anal., 21, 1990, 823-836.

[3] A. Ávila, G. Griso, B. Miara. *Bandes phononiques interdites en élasticité linéarisée*, C. R. Acad. Sci. Paris, Ser. I 340, 2005, 933-938.

[4] G. Bouchitté, D. Felbacq. *Homogenization near resonances and artificial magnetism from dielectrics*, C. R. Acad. Sci. Paris, Ser. I 339, 2004, 377-382.

[5] A. Cioranescu, A. Damlamian, G. Griso. *Periodic unfolding and homogenization*. C. R. Acad. Sci. Paris, Ser. I 335 (2002) 99-104.

[6] A. Damlamian. *An elementary introduction to Periodic Unfolding*. GAKUTO International series Math. Sci. Appl. Vol. 24, (2005) Multi scale problems and Asymptotic Analysis, 119-136.

[7] J.S. Jensen, N.L. Pedersen. *On maximal eigenfrequency separation in two-material structures: The 1D and 2D scalar cases*, Journal of Sound and Vibration 289 (2006) 967-986.

[8] G. Nguetseng. *A general convergence result for a functioanl related to the theory of homogenization*, SIAM J. Math. Anal., 20 (3), (1989), 608-623.

[9] B. Miara, E. Rohan, *Shape optimization of phononic materials*. 77th Annual Meeting of the Gesellschaft für Angewandte Mathematik und Mechanik e.V. (GAMM), Berlin, 27-31 March 2006.

[10] J.B. Pendry, *J. Mod. Optics* 41 209, (1993).

[11] E. Rohan, B. Miara, *Microstructural sensitivity of acoustic band gaps*. 17th IMACS World Congress, Paris 11-15 July 2005.

[12] O. Sigmund, J. S. Jensen, *Systematic design of phononic band-gap materials and structures by topology optimization*, Phil. Trans. R. Soc. London, A (2003) 361, 1001-1019.

[13] J. Vasseur, P. Deymier, G. Frantziskonis, G. Hong, B. Djafari-Rouhani, L. Dobrzynski. *Experimental evidence for the existence of absolute acoustic band gaps in two-dimensional periodic composite media*, J. Phy. Condens. Matter 10 (1998) 6051-6064.

[14] E. Yablonovitch, *J. Phys. Condens. Matter* 5 2443, (1993).